# A CMOS Microelectrode Array Integrated into an Open, Continuously Perfused Microfluidic System

**Conference Paper**

**Author(s):**
Bounik, Raziyeh; Lee, Jihyun; Viswam, Vijay; Cardes Garcia, Fernando (ID); Modena, Mario M.; Hierlemann, Andreas (ID)

# A CMOS Microelectrode Array Integrated into an Open, Continuously Perfused Microfluidic System

Raziyeh Bounik[1], Jihyun Lee[1], Vijay Viswam[1,2], Fernando Cardes[1], Mario M. Modena[1], and Andreas Hierlemann[1]

[1] ETH Zürich, Department of Biosystems Science and Engineering, Basel, Switzerland

[2] MaxWell Biosystems AG, Zürich, Switzerland

Raziyeh.bounik@bsse.ethz.ch*

*Abstract*— A monolithic device is presented that features a CMOS microelectrode array system integrated into an open microfluidic device. The system includes two microelectrode arrays, each featuring 1024 microelectrodes arrayed within a $1.6 \times 1.6$ mm² sensing area. It enables label-free *in vitro* impedance and electrophysiology recordings from cells and tissues. The open microfluidic system provides oxygenation and perfusion capabilities, as well as controllable liquid handling, which makes the device a versatile tool for long-term experiments and compound development studies.

*Keywords*— *CMOS microelectrode array (MEA); electrophysiology; impedance spectroscopy; open microfluidic system;*

## I. INTRODUCTION

Microelectrode arrays (MEAs) are extensively used in *in vitro* studies to measure electrical features of cells and tissues. MEAs have been mainly used to record the electrical activity of electrogenic cells, such as neurons or cardiac cells [1]–[3], to characterize the morphology and adhesion of cells and tissues by impedance spectroscopy [4]–[6], to monitor the concentration of specific analytes and neurotransmitters [7], [8], and for optical detection and thermal monitoring [9].

Introduction of complementary metal oxide semiconductor (CMOS)-based MEA systems enabled to fabricate high-density MEAs that can perform low-noise recordings and include multiple functionalities on a single chip [10], [11]. However, current MEA systems are designed to be operated under static conditions within a comparably large medium volume. Static cell or tissue culturing increases the risk of contamination, e.g., during medium exchange and limits the scope of drug testing experiments depending on the applied methods [12]. Here, we propose a route to integrating MEA systems with dynamic cell culture systems, such as microfluidic systems, which are of great interest, as the cells or tissue culture constantly receive fresh medium and can be exposed to dynamic drug profiles by using a perfusion apparatus [13].

We present a new CMOS-MEA-based device that is integrated into an open microfluidic system. Our CMOS-MEA chip can be used to perform electrophysiology and impedance recordings. The microfluidic system enables continuous perfusion and drug dosage, which better mimic in-vivo conditions. Small medium volumes (few tens of μl) ensure precise liquid control for, e.g., dynamic drug testing scenarios. The open microfluidic design provides sufficient oxygen exchange for ensuring cell viability and offers easy transfer and recovery of cells and tissues from the MEA surface.

## II. DEVICE DESCRIPTION

The device consists of two main components: (1) a high-density CMOS-MEA chip and (2) an open microfluidic system. A glass substrate is employed as a solid support for the microfluidic system and the MEA chip. The glass substrate features platinum patterns to connect the signal and supply lines of the MEA chip to the off-chip measurement setup (Fig. 1A).

The CMOS-MEA chip includes two electrode arrays. Each array contains 1024 electrodes and is connected to 64 electrophysiology and eight impedance recording channels on chip (Fig. 1B). The circuitry of the electrophysiology and impedance recording channels are similar to those published in [10].

The electrophysiology channels are implemented as four-stage amplifiers, with a programmable gain ranging from 29 dB to 76 dB, and band-pass filters, with a bandwidth from 0.4 Hz to 6.6 kHz. Each channel features individual continuous-time first- and second-stage amplifiers; every eight channels share eight switched-capacitor (SC) third-stage amplifiers, and all 64 channels share one SC fourth-stage amplifier. A programmable gain is essential to accommodate the different signal levels that various types of electrogenic cells can generate, ranging from small neural action potentials (tens of $\mu V_{pp}$) to large cardiac action potentials (several $mV_{pp}$) [14]. Filters are required to cancel offsets and slow voltage drifts, which would saturate amplifiers, and to attenuate high-frequency signals before sampling to prevent aliasing. After filtering and amplification, signals are digitized by a 10-bit successive-approximation-register (SAR) ADC with serial output. The ADC operates at 1.28 MS/s, sampling each of the 64 channels at 20 kS/s.

The impedance recording channels are designed based on a lock-in detection scheme. A sinusoidal stimulus voltage, generated on-chip, is applied between the reference electrode and the target working electrodes. The resulting currents are sensed by eight transimpedance amplifiers (TIAs), and mixed with the on-chip generated synchronous in-phase (I) and quadrature (Q) square signals to generate I/Q demodulated impedance signals. These signals are then low-pass filtered to remove the high-frequency harmonics, afterwards multiplexed and digitized by two delta-sigma ADCs. The cut-off frequency of the low-pass filter is 16 kHz, and the
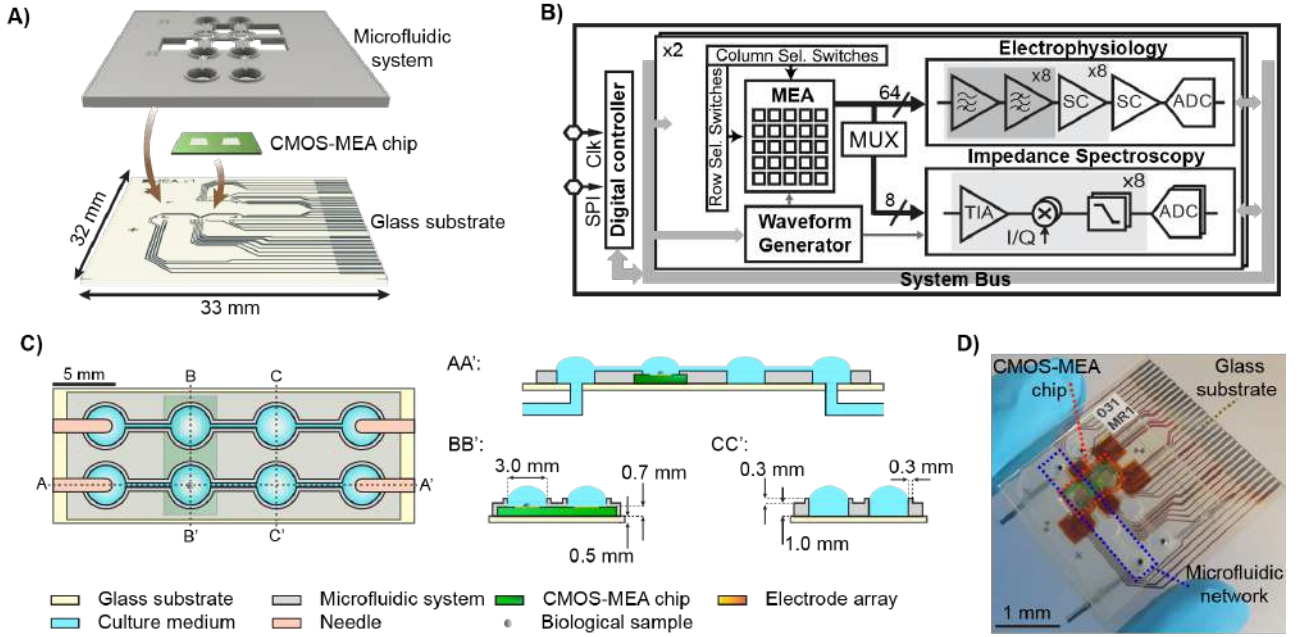
Fig. 1. A) Main components of the device. B) Schematic overview of the CMOS-MEA chip. C) Design details of the microfluidic system (top view and side views). D) Photograph of the assembled system.

sampling frequency of the ADCs is 1.28 MHz. The dynamic range of the impedance

spectroscopy module ranges between 1 Hz and 1 MHz. Including two MEAs on a single chip facilitates parallelization of experiments and a reduction of the required wiring in comparison to using two individual MEA chips.

The microfluidic arrangement contains two fluidic networks, each consisting of four compartments. Two compartments are connected to the fluidic inlets and outlets, one compartment is aligned with the corresponding MEA on the CMOS chip to host the sample of interest, and the fourth compartment can be used for liquid control if needed. The liquid volume in each compartment was 13.5 µl, with the exception of the compartment on top of the CMOS-MEA chip, which included 8.5 µl (Fig. 1C).

## III. DEVICE FABRICATION

The CMOS-MEA chip was fabricated in 0.18 µm CMOS technology with a die size of $4 \times 9$ mm$^2$. Pt electrodes were deposited during CMOS postprocessing on wafer level to define the actual size of the electrodes, which was $38 \times 42$ µm$^2$. A summary of the features of the CMOS-MEA chip is presented in Table I.

The microfluidic system was fabricated using polydimethylsiloxane (PDMS) by soft lithography through a double-sided molding process, where a 3D-printed mold (printed in ceramic-like Perform, Protolabs, Feldkirchen, Germany) and a silanized PDMS mold were employed as the bottom and top mold, respectively. The microfluidic system was assembled with the CMOS-MEA chip through the following main steps: (1) the CMOS-MEA chip was affixed on the glass substrate by using a bio-compatible epoxy; (2) 1-mm openings were drilled in the glass at the center of the inlet and outlet compartments; (3) the microfluidic system was plasma-bonded onto the glass substrate and CMOS-MEA chip; (4) wire-bonding of the CMOS-MEA chip to the glass

substrate was performed, followed by a protection of the bond-wires with a bio-compatible epoxy; (5) fluidic inlets and outlets were implemented by inserting metal needles, which were attached and held in position by a 2-mm layer of PDMS (Fig. 1D).

TABLE I. OVERVIEW OF THE CMOS-MEA CHIP

| CMOS-MEA chip | |
| --- | --- |
| Technology | 0.18 µm CMOS |
| No. of arrays | 2 |
| Sensing area per array | 1.6 mm × 1.6 mm |
| No. of electrodes per array | 1024 |
| Electrode size / material | 38 µm × 42 µm / Pt |
| **Electrophysiology channels** | |
| No. of channels per array | 64 |
| Gain | 29 – 76 dB |
| Power consumption per channel | 24 µW |
| **Impedance recording channels** | |
| No. of channels per array | 8 |
| Frequency range | 1 Hz – 1 MHz |
| Power consumption per channel | 385 µW |

## IV. MEASUREMENT RESULTS

A custom-made C# program was developed to generate the system control commands and send them to the CMOS-MEA chip through a serial peripheral interface (SPI). The serial output data of both MEAs were recorded by using a data acquisition card (DAQ) (PXIe-6537, National Instruments, Austin, United States) and a custom-made LabVIEW program. neMESYS syringe pumps (Cetoni GmbH, Korbussen, Germany) were employed to precisely control the fluidic flow.

First, the electrical characterization of the CMOS-MEA chip was conducted. The results of one of the equivalent arrays are presented here. The gain and input-referred offset of the electrophysiology channels were measured as $75.4 \pm 0.1$ dB and $-0.004 \pm 0.005$ mV by applying a common sinusoidal signal to all channels. The spread of the maximum gain and input-referred offset are shown in Fig. 2A. Impedance
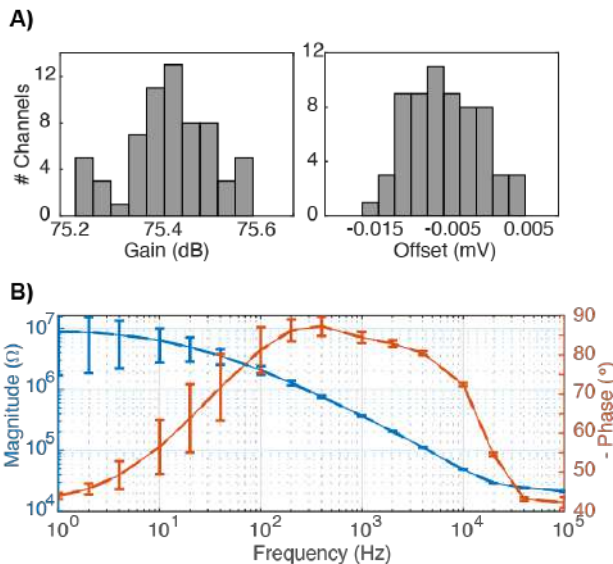
Fig. 2. A) Spread of gain and input-referred offset between 64 electrophysiology recording channels; B) Impedance spectroscopy of electrodes in PBS.

spectroscopy measurements of electrodes were conducted in phosphate-buffered saline solution (PBS), where a dominance of the charge transfer resistor, the double-layer capacitor and the spreading resistor were distinguishable at low (< 10 Hz), mid-range, and high (> 10 kHz) frequencies (Fig. 2B).

To investigate the impedance-recording performance of the channels, impedance imaging of glass beads (Fig.3A) was done. Glass beads have impedance features similar to some biological tissues, as they are non-conductive and block the current. Glass beads of 400 µm and 700 µm in diameter were used. Fig. 3B shows the impedance magnitude and phase data acquired at three frequencies. It can be seen that at low (1 kHz) frequency, the difference in impedance caused by glass beads was very small compared to the initial high electrode impedance, so that the position of the beads was not detectable. As the frequency increased, and – concurrently - the electrode impedance decreased, the relative change in impedance caused by the beads was higher. At 10 kHz, the position of the beads and the difference in their size became clearly visible. At 100 kHz, the size of the beads could be estimated with larger precision, especially by using the impedance phase data.

To show the effectiveness of the integrated open microfluidic system, the effect of epinephrine on iPSC-derived cardiac microtissues was examined. The human induced pluripotent stem cell (hiPSC) line, CW30318CC1 (Fujifilm Cellular Dynamics, Inc., Madison, WI, USA), originally derived from a healthy donor, was differentiated into cardiomyocytes [15]. The beating cardiomyocytes were then dissociated from the culture dish and seeded into low-adhesion, U-bottom, 96-well plates to form spherical microtissues. To conduct the experiment, the fluidic compartments were loaded with culture medium through the connected syringes. Then, iPSc-derived cardiac microtissues were harvested from the culture well-plate, and directly transferred onto one MEA (Fig. 4A). Constant perfusion, with an inflow and outflow of ±2.5 µl/min, was applied to provide fresh nutrients to the microtissue during the experiments.
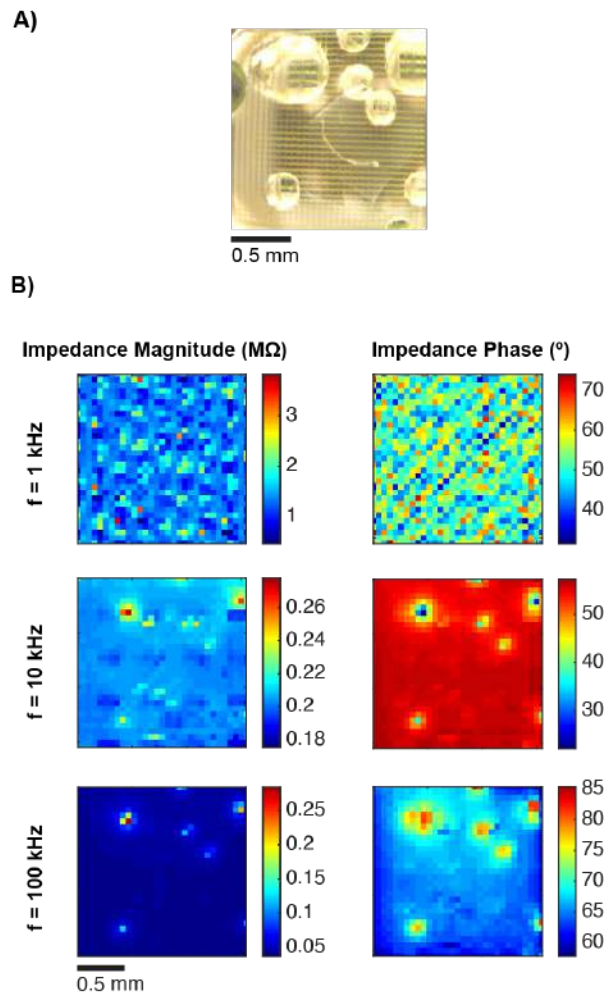




Fig. 3. A) Glass beads of different sizes on one array; B) Impedance images of the glass beads at three different frequencies.

Electrophysiology recordings from the electrodes below the beating microtissue indicated an average beating rate of 45 min$^{-1}$. Then, 10 µM epinephrine were applied through the fluidic inlet. Electrophysiology recordings showed an increase in amplitude and beating frequency (72 min$^{-1}$) of the cardiac microtissue shortly after the epinephrin arrived at the MEA (Fig. 4B).

## V. CONCLUSION

In this paper, we presented a new device combination comprising a CMOS-MEA chip and an open microfluidic system. The CMOS-MEA chip included two MEAs, with 1024 microelectrodes to conduct electrophysiology and impedance recordings. We demonstrated the functionalities of the device by impedance imaging of different-size glass beads and electrophysiological recordings of the beating of cardiac microtissues, as well as epinephrine dosage through the the integrated microfluidic system. The open microfluidic system provides better oxygenation and enables to directly transfer and harvest the samples to and from the MEA. Applying constant perfusion through the integrated microfluidic system more faithfully recapitulates the in-vivo situation by providing constant flow and fresh medium to the microtissue. Furthermore, perfusion helps to avoid up-concentration of salts and waste products near the tissue in the medium, which

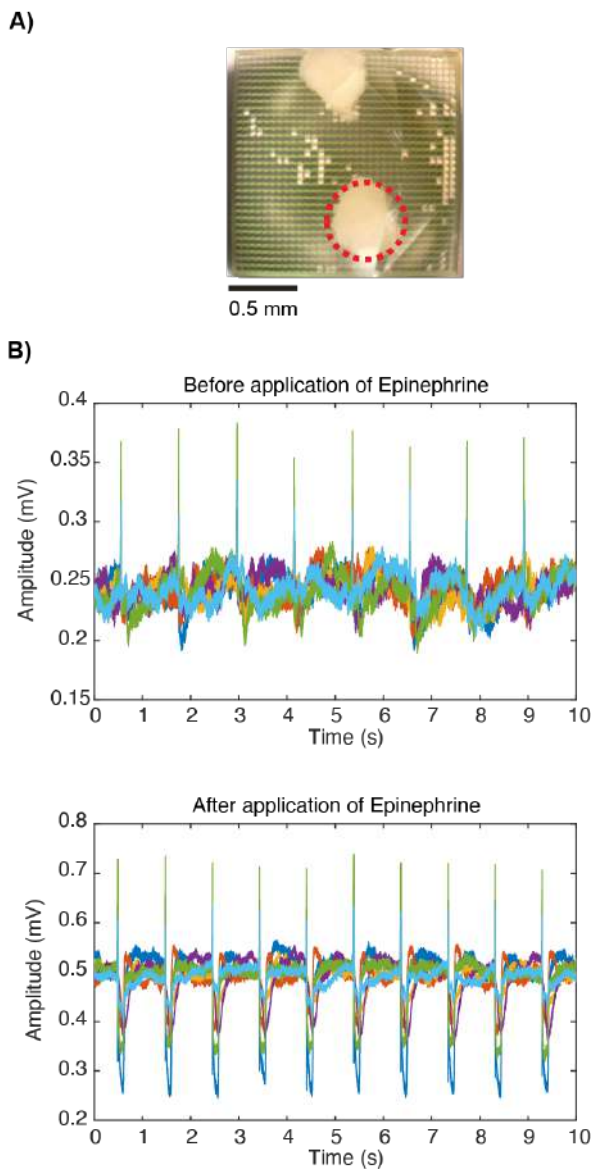would impact culturing of microtissues in small medium volumes.



Fig. 4. A) iPSC-derived cardiac microtissues on one array; B) electrophysiology recordings of the electrodes covered by the cardiac microtissue, before and after application of Epinephrine.

REFERENCES

[1] X. Yuan et al., "Versatile live-cell activity analysis platform for characterization of neuronal dynamics at single-cell and network level," Nat. Commun., vol. 11, no. 1, 2020, doi: 10.1038/s41467-020-18620-4.

[2] H. Shin, S. Jeong, J. H. Lee, W. Sun, N. Choi, and I. J. Cho, "3D high-density microelectrode array with optical stimulation and drug delivery for investigating neural circuit dynamics," Nat. Commun., vol. 12, no. 1, pp. 1–18, 2021, doi: 10.1038/s41467-020-20763-3.

[3] V. Emmenegger, M. E. J. Obien, F. Franke, and A. Hierlemann, "Technologies to study action potential propagation with a focus on HD-MEAs," Front. Cell. Neurosci., vol. 13, no. April, pp. 1–11, 2019, doi: 10.3389/fncel.2019.00159.

[4] F. Widdershoven et al., "A CMOS Pixelated Nanocapacitor Biosensor Platform for High-Frequency Impedance Spectroscopy and Imaging," IEEE Trans. Biomed. Circuits Syst., vol. 12, no. 6, pp. 1369–1382, 2018, doi: 10.1109/TBCAS.2018.2861558.

[5] V. Viswam et al., "Impedance Spectroscopy and Electrophysiological Imaging of Cells with a High-Density CMOS Microelectrode Array System," IEEE Trans. Biomed. Circuits Syst., vol. 12, no. 6, pp. 1356–1368, 2018, doi: 10.1109/TBCAS.2018.2881044.

[6] R. Bounik, F. Cardes, H. Ulusan, M. M. Modena, and A. Hierlemann, "Impedance Imaging of Cells and Tissues: Design and Applications," BME Front., vol. 2022, pp. 1–21, Jun. 2022, doi: 10.34133/2022/9857485.

[7] J. Rothe, O. Frey, A. Stettler, Y. Chen, and A. Hierlemann, "Fully integrated CMOS microsystem for electrochemical measurements on 32 ?? 32 working electrodes at 90 frames per second," Anal. Chem., vol. 86, no. 13, pp. 6425–6432, 2014, doi: 10.1021/ac500862v.

[8] W. Tedjo and T. Chen, "An Integrated Biosensor System with a High-Density Microelectrode Array for Real-Time Electrochemical Imaging," IEEE Trans. Biomed. Circuits Syst., vol. 14, no. 1, pp. 20–35, 2020, doi: 10.1109/TBCAS.2019.2953579.

[9] T. Chi et al., "A Multi-Modality CMOS Sensor Array for Cell-Based Assay and Drug Screening," IEEE Trans. Biomed. Circuits Syst., vol. 9, no. 6, pp. 801–814, Dec. 2015, doi: 10.1109/TBCAS.2015.2504984.

[10] J. Dragas et al., "In Vitro Multi-Functional Microelectrode Array Featuring 59 760 Electrodes, 2048 Electrophysiology Channels, Stimulation, Impedance Measurement, and Neurotransmitter Detection Channels," IEEE J. Solid-State Circuits, vol. 52, no. 6, pp. 1576–1590, 2017, doi: 10.1109/JSSC.2017.2686580.

[11] C. M. Lopez et al., "A multimodal CMOS MEA for high-throughput intracellular action potential measurements and impedance spectroscopy in drug-screening applications," IEEE J. Solid-State Circuits, vol. 53, no. 11, pp. 3076–3086, 2018, doi: 10.1109/JSSC.2018.2863952.

[12] P. M. Misun, J. Rothe, Y. R. F. Schmid, A. Hierlemann, and O. Frey, "Multi-analyte biosensor interface for real-time monitoring of 3D microtissue spheroids in hanging-drop networks," Microsystems Nanoeng., vol. 2, no. October 2015, p. 16022, 2016, doi: 10.1038/micronano.2016.22.

[13] J. El-Ali, P. K. Sorger, and K. F. Jensen, "Cells on chips," Nature, vol. 442, no. 7101, pp. 403–411, 2006, doi: 10.1038/nature05063.

[14] M. Ballini et al., "A 1024-channel CMOS microelectrode array with 26,400 electrodes for recording and stimulation of electrogenic cells in vitro," IEEE J. Solid-State Circuits, vol. 49, no. 11, pp. 2705–2719, 2014, doi: 10.1109/JSSC.2014.2359219.

[15] M. Zhao, Y. Tang, Y. Zhou, and J. Zhang, "Deciphering Role of Wnt Signalling in Cardiac Mesoderm and Cardiomyocyte Differentiation from Human iPSCs: Four-dimensional control of Wnt pathway for hiPSC-CMs differentiation," Sci. Rep., vol. 9, no. 1, pp. 1–15, 2019, doi: 10.1038/s41598-019-55620-x.